C. R. Palevol 12 (2013) 293–304

Contents lists available at ScienceDirect

Comptes Rendus Palevol

www.sciencedirect.com

Human paleontology and prehistory (Palaeoanthropology)

Endostructural characterization of the *H. heidelbergensis* dental remains from the early Middle Pleistocene site of Tighenif, Algeria

Caractérisation de l'endostructure des restes dentaires de H. heidelbergensis *du site pléistocène moyen initial de Tighenif, Algérie*

Clément Zanolli[a,b,*], Arnaud Mazurier[c]

[a] *Multidisciplinary Laboratory, International Centre for Theoretical Physics, Trieste, Italy*
[b] *Département de préhistoire, UMR 7194, MNHN, Paris, France*
[c] *Société études recherches matériaux, CRI-BIOPOLE, 4, rue Carole-Heitz, 86000 Poitiers, France*

ARTICLE INFO

Article history:
Received 9 February 2013
Accepted after revision 22 June 2013
Available online 13 August 2013

Presented by Philippe Taquet

Keywords:
Tighenif
Permanent teeth
Structural morphology
Tissue proportions
Early Middle Pleistocene
H. heidelbergensis
Algeria

Mots clés :
Tighenif
Dents permanentes
Morphologie structurale
Proportions des tissus
Pléistocène moyen initial
H. heidelbergensis
Algérie

ABSTRACT

The early Middle Pleistocene human fossil assemblage from Tighenif, Algeria, likely samples some among the earliest representatives of the *Homo heidelbergensis* morph. A previous study of three deciduous molars from this assemblage revealed an inner structural signature (crown tissue proportions and enamel thickness topography) roughly approximating the modern human figures. By using advanced techniques of microtomographic-based 3D virtual imaging and quantitative analysis, we significantly extend here the currently available record to 22 permanent teeth, mostly from the mandibular dentition, and provide the first detailed description of the structural condition characterizing this North African deme near the Lower-Middle Pleistocene boundary. Together with a certain degree of individual variation, the teeth of Tighenif exhibit a structural pattern combining primitive, derived, and unique features. The lower molars display a set of enamel-dentine junction nonmetric traits more frequently found in recent humans than in Neanderthals, but also a blend of Neanderthal- and modern-like characteristics in terms of structural conformation and crown tissue proportions. They also exhibit relatively large pulp cavities, with a rather high root bifurcation and well-separated pulp canals, a pattern more closely approximating the condition reported for Late Pleistocene Aterians.

RÉSUMÉ

L'assemblage humain fossile du site pléistocène initial de Tighenif, en Algérie, compte vraisemblablement parmi les premiers représentants du morphe *Homo heidelbergensis*. Une précédente étude de trois molaires déciduales de cet assemblage a révélé une signature structurale interne (proportions des tissus de la couronne et topographie de l'épaisseur de l'émail) approchant le schéma humain moderne. En utilisant des techniques avancées d'imagerie virtuelle et d'analyse quantitative 3D basées sur la microtomographie, nous étendons ici de manière significative le registre actuellement disponible à 22 dents permanentes, principalement de la denture mandibulaire, et fournissons les premières descriptions détaillées de la condition structurale caractérisant cette population

* Corresponding author. Multidisciplinary Laboratory, International Centre for Theoretical Physics, Trieste, Italy.
E-mail address: clement.zanolli@gmail.com (C. Zanolli).

1631-0683/$ – see front matter
http://dx.doi.org/10.1016/j.crpv.2013.06.004

Nord-Africaine, autour de la limite Pléistocène inférieur-moyen. Malgré un certain degré de variation individuelle, les dents de Tighenif montrent un patron structural combinant des caractéristiques primitives, dérivées et uniques. Les molaires inférieures dévoilent au niveau de la jonction émail-dentine un ensemble de traits non métriques plus fréquemment trouvés chez les humains modernes que chez les Néandertaliens, mais aussi un mélange de caractéristiques semblables soit à celles des Néandertaliens, soit à celles des humains modernes en termes de conformation structurale et de proportions des tissus. Elles présentent aussi des cavités pulpaires volumineuses, avec une bifurcation radiculaire assez élevée et des canaux pulpaires bien séparés, s'approchant plus particulièrement de la condition rapportée pour des Atériens du Pléistocène supérieur.

1. Introduction

The early Middle Pleistocene human remains from the site of Tighenif (also known as Ternifine, formerly Palikao) were discovered between 1954 and 1956 in a sand quarry in the province of Mascara, Algeria (Arambourg, 1954, 1955, 1957; Arambourg and Hoffstetter, 1954). Based on comparative biochronology, the site is currently dated to ca. 700 kyr (Geraads et al., 1986). The fossil collection consists of nine isolated teeth (three deciduous and six permanent), two nearly complete adult mandibles (Tighenif 1 and 3), one adult hemi-mandible (Tighenif 2), and a parietal fragment (Tighenif 4). As a whole, the dental record suggests a minimum of five individuals, notably of one child and four adults (Arambourg and Hoffstetter, 1963; Schwartz and Tattersall, 2003; Tillier, 1980).

Originally attributed to *Atlanthropus mauritanicus* (Arambourg, 1954, 1955), the fossil assemblage from Tighenif has been later on commonly integrated within the *Homo erectus* hypodigm, notably because of some similarities with the Chinese dentognathic material from Zhoukoudian (Howell, 1960; Le Gros Clark, 1964; Rightmire, 1990; Tillier, 1980; for a review: Antón, 2003; Antón et al., 2007; Schwartz and Tattersall, 2003). While some dental crown features have also suggested its possible affinity to the morph represented by the Early Pleistocene specimens from Gran Dolina, Spain (Schwartz and Tattersall, 2005), the morphometric study of a newly discovered *H. antecessor* mandibular fragment has revealed a symphyseal and premolar morphology distinct from the condition characterizing the Algerian specimens (Bermúdez de Castro et al., 2011).

A recent revision of the *Homo heidelbergensis* hypodigm (Mounier et al., 2009) convincingly suggests that the amount of morphological and dimensional similarities shown by the assemblage from Tighenif grants its allocation to this taxon (Stringer, 2012). Additionally, the same study (Mounier et al., 2009) pointed out that, because of some derived features such as the development of a chin-like protuberance on Tighenif 2 (Schwartz and Tattersall, 2000, 2010), the Algerian material is morphologically closer to *H. sapiens* than to the Neanderthals, a conclusion also partially supported by an independent microtomographic-based analysis of the inner structural organization of three upper deciduous molars (Zanolli et al., 2009, 2010).

By using advanced techniques of three-dimensional high-resolution virtual imaging and quantitative characterization (Bayle et al., 2010; Bondioli et al., 2010; Macchiarelli et al., 2008, 2009, 2013; Olejniczak et al., 2008a, 2008b; Skinner et al., 2008; Zanolli et al., 2012), we present here original evidence on the inner structural features of 22 permanent elements from this exceptional dental sample and, on comparative grounds, provide the first description of the condition characterizing North African *H. heidelbergensis* near the Lower-Middle Pleistocene boundary.

2. Materials and methods of analysis

In this study we consider 22 permanent teeth selected from the dentognathic fossil material of Tighenif. In the text, tables and captions, the type, position, and laterality of the teeth have been systematically indicated as follows: I1, central incisor; I2, lateral incisor; C, canine; P3, third premolar; P4, fourth premolar; M1, first molar; M2, second molar; M3, third molar; L, lower; U, upper; L, left; R, right. More specifically, the investigated sample includes six isolated specimens (LRI1, LRI2, LLC, URM1/2, and two undetermined upper molars, respectively representing the fragmentary crown of an unworn URM, and an extremely worn ULM) and the 16 teeth virtually extracted from the mandibles Tighenif 1 (RI2 [crown missing most of the labial aspect], RP3-M3, LP3-M3) and Tighenif 2 (LP3-M3) (Fig. 1). Conversely, the teeth from Tighenif 3 have not been included in the analysis because of their advanced degree of occlusal wear.

Between July 2009 and October 2010, the isolated tooth specimens and the mandibles Tighenif 1 and 2 have been imaged by microtomography (μCT) at the Centre de Microtomographie of the University of Poitiers. The acquisitions were realized with a X8050-16 Viscom AG equipment (camera 1004 × 1004) according to the following parameters: 115 to 125 kV voltage; 0.35 to 0.60 mA current; a projection each 0.20° to 0.25°. The final volumes were reconstructed using DigiCT v.2.3.3 (DIGISENS) in 8-bit format, with an isotropic voxel size ranging from 21.57 to 49.17 μm.

Using Amira v.5.3 (Visualization Sciences Group Inc.) and ImageJ v.1.46 (NIH; Schneider et al., 2012), a semi-automatic threshold-based segmentation has been carried out following the half-maximum height method (HMH; Spoor et al., 1993) and the region of interest thresholding protocol (ROI-Tb; Fajardo et al., 2002), taking repeated measurements on different slices of the virtual stack (Coleman and Colbert, 2007).

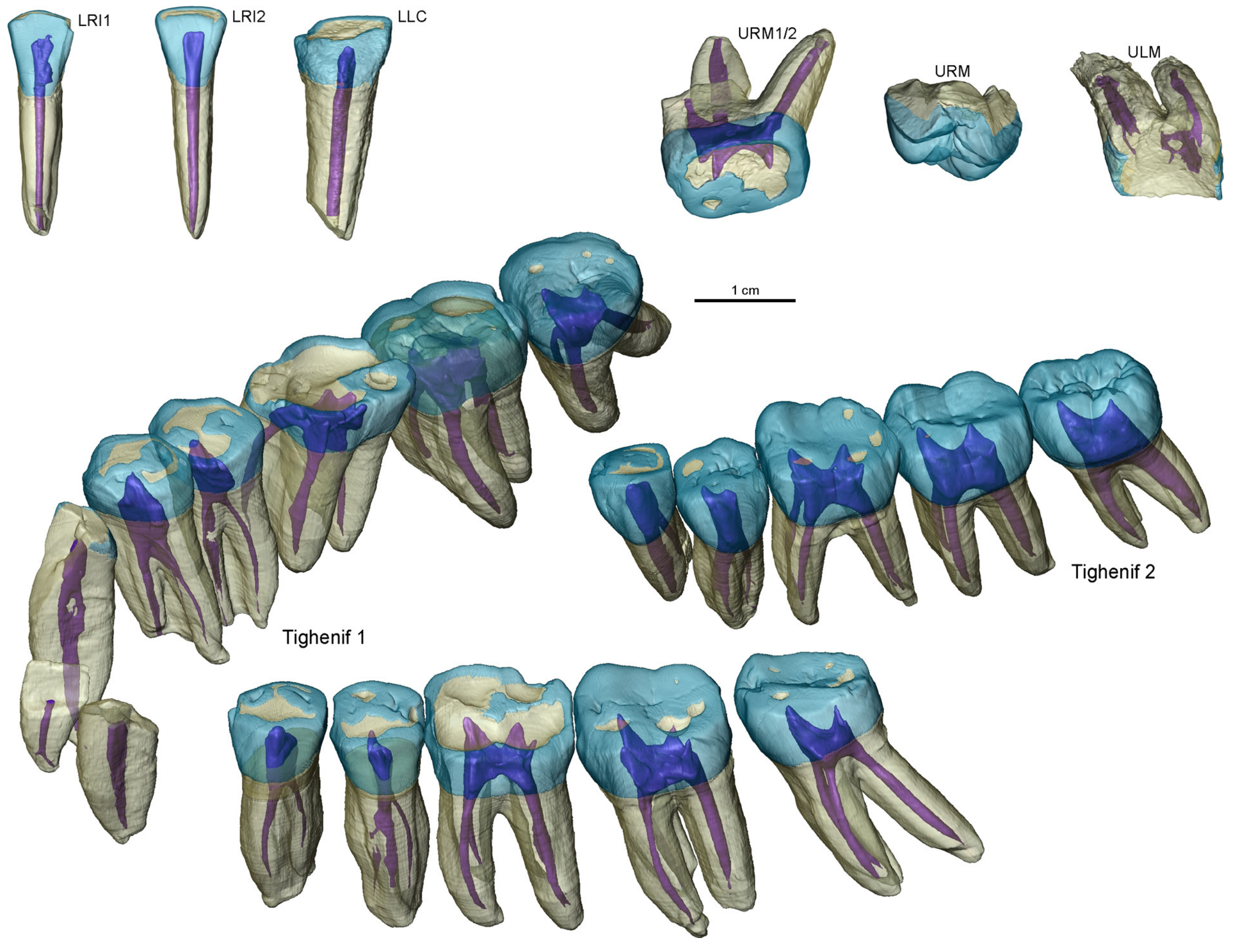

Fig. 1. Microtomographic-based 3D reconstruction of six isolated teeth from Tighenif (top) and of the virtually extracted tooth elements from the mandibles Tighenif 1 (left) and 2 (right), with the enamel and dentine rendered in transparency thus highlighting the pulp cavities. In Tighenif 1, the virtually extracted root fragments residual of the LRI1 and LLI2 are also shown. Colour available online.

Fig. 1. Reconstruction microtomographique 3D de six dents isolées de Tighenif (haut) et des éléments dentaires virtuellement extraits des mandibules Tighenif 1 (gauche) et 2 (droite), avec l'émail et la dentine en transparence, permettant ainsi la visualisation de leurs cavités pulpaires. Chez Tighenif 1, les fragments virtuellement extraits de racine de la LRI1 et de la LLI2 sont aussi montrés. Couleur disponible en ligne.

Depending on the degree of occlusal wear (assessed following Smith, 1984) and general preservation conditions of each tooth element, the following variables describing tissue proportions were digitally measured or calculated: V_e, the volume of the enamel cap (mm^3); V_d, the total volume of dentine (mm^3); V_p, the total volume of pulp (mm^3); V_t, the total tooth volume (mm^3); V_p/V_t (= 100*V_p/V_t), the percent of pulp with respect to the total tooth volume (%); V_{cd}, the volume of the coronal dentine (mm^3); V_{cp}, the volume of the coronal pulp (mm^3); V_{cdp}, the volume of the coronal dentine, including the coronal aspect of the pulp chamber (mm^3); V_c, the total crown volume, including enamel, dentine, and pulp (mm^3); SEDJ, the enamel-dentine junction (EDJ) surface (mm^2); V_{cdp}/V_c (= 100*V_{cdp}/V_c), the percent of coronal volume that is dentine and pulp (%); 3D AET (= V_e/SEDJ), the three-dimensional average enamel thickness (mm); 3D RET (= 100*3D AET/($V_{cdp}{}^{1/3}$)), the scale-free three-dimensional relative enamel thickness (Kono, 2004; Olejniczak et al., 2008a).

The presence of some nonmetric features at the EDJ has been scored following Skinner et al. (2008) for the accessory cusps and Bailey et al. (2011) for the mid-trigonid crest.

Intra- and interobserver tests for accuracy of the microtomographic-based measures run by two observers revealed differences inferior to 4%.

For some of the variables listed above, the results from the LM2 and LM3 of Tighenif 2, i.e., the least worn teeth, have been compared to the evidence available for: Neanderthals (NEA; Kupczik and Hublin, 2010; Macchiarelli et al., 2013; NESPOS Database, 2013; Olejniczak et al., 2008a); fossil modern humans from Aterian Moroccan sites (AFMH; Kupczik and Hublin, 2010); and extant humans (EH; Kupczik and Hublin, 2010; Olejniczak et al., 2008b; and original data) (Table S1 in Supplementary data).

Adjusted Z-score analyses (Maureille et al., 2001; Scolan et al., 2011) were performed for three variables expressing tooth tissue proportions on the LM2s and LM3s. This statistical method allows the comparison of unbalanced samples, often limitative for the fossil record, using the Student's t inverse distribution following the formula: $[(x-m)/(s^*\mathrm{sqrt}(1+1/n))]/(\mathrm{Student.t.inverse}(0.05; n-1))$, where x is the value of the variable; m is the mean of the same variable for a comparative sample; n is the size of the comparative sample for this variable; and s is its standard deviation for the comparative sample.

Geometric morphometric analyses (GMA) of the EDJ were performed on the unsmoothed reconstructed virtual surfaces of the LM2s and LM3s by placing a total of seven landmarks on the apex of the protoconid, metaconid, entoconid and hypoconid, and at each intermediate lowest point between two dentine horns along the dentine marginal ridge, except between the two distal horns (because of the variable presence of the hypoconulid, this latter cusp and the distal marginal distal ridge were not considered). However, while the EDJ morphology is not affected by occlusal wear in Tighenif 2 molars, this is not the case for the LRM3 in Tighenif 1, whose buccal cusp apex and dentine horn extremities have been virtually integrated based on the intact Tighenif 2 reference specimen.

By using the package Morpho 0.23.3 (Schlager, 2013) for R v.2.15.2 (R Development Core Team, 2013), we performed a generalized Procrustes analysis (GPA) and a between-group principal component analysis (bgPCA) based on the Procrustes shape coordinates (Mitteroecker and Bookstein, 2011). A 10,000 iterations permutations test allowed the statistically assessment of inter-group differences. For the specific purposes of this analysis, the comparative sample included 12 Neanderthal molars from Regourdou and Krapina (NEA [7 LM2 and 5 LM3]; NESPOS Database, 2013) and 26 extant human molars (EH [17 LM2 and 9 LM3]; original data) (Table S1 in Supplementary data). Because the bgPCA analysis needs more than two individuals per group to be performed, the available LM2s and LM3s have been pooled.

3. Results

Following the preliminary phases of 3D reconstruction and individual virtual extraction of each tooth element still preserved in situ in the two adult mandibles, we noticed the previously unreported presence of a local decalcification affecting the distal crown aspects of the LLP4, in Tighenif 2, and of the LRM1, in Tighenif 1. These lesions, respectively representing a relatively shallow but extended depression ($\sim$6.7 mm^3) and a deeper subspherical cavity ($\sim$5.0 mm^3), distinctly involve both enamel and dentine, but do not reach the pulp cavity (Fig. 2). Because of their location and shape, as well as of the quality and preservation conditions of the surrounding mineralized tissues, we consider these features as representing interproximal carious lesions of stage 5 (Hillson, 2001), likely unnoticed in previous studies because masked in both cases by the close contact with the mesial margin of the corresponding distal crown.

3.1. Outer vs. inner structural morphology

In all investigated cases, the comparison between the outer enamel surface (OES) and the topography of the enamel-dentine junction (EDJ) has revealed a substantial morphostructural adequacy between the features developed at the two interfaces (Figs. 1 and 3).

The crown of the isolated LRI1 shows flat lingual and labial outer surfaces, without any expression of marginal ridges or *tuberculum dentale*, the same morphology appearing at the EDJ level. Its root (Fig. 1) is compressed mesiodistally, with a large but shallow longitudinal groove on both mesial and distal aspects (Arambourg and Hoffstetter, 1963), whereas the pulp cavity exhibits a spatula-like shape, turning into an ovoid outlined canal at root level.

The isolated LRI2 presents a structural morphology close to that found in the LRI1, except that here the marginal ridges are slightly developed and that the external distal longitudinal root groove is only barely perceptible. In this case, the shape of the relatively large root cavity also shows an ovoid contour.

Despite its advanced occlusal wear, the marked marginal ridges and a weak expression of the *tuberculum dentale* are recognizable on the isolated LLC. While apically fractured, its root and inner pulp cavity (Fig. 1) are mesiodistally compressed and exhibit a relatively deep longitudinal groove on the mesial aspect.

The three available LP3s present an asymmetric bicuspid outer crown with deep anterior and posterior foveae separated by a high transversal crest (Arambourg and Hoffstetter, 1963), a morphology also clearly expressed at the EDJ level (Fig. 3). Externally, in both Tighenif 1 and 2, the LP3 root is constituted by three fused branches separated by longitudinal grooves, two with a free apex at the buccal and lingual level, and a third, shorter, coalesced in mesiobuccal position (Fig. 1). However, the inner structure reveals three root pulp canals, including a modestly mesiobuccally developed and two larger radicals in the mesial and distal branches, expressing a C-shaped cross-section typical of the Tomes' root 2R morphology of grade 4 (Turner II et al., 1991; Wood et al., 1988).

As a whole, the LP4s display a moderate degree of wear, which allowed the identification of two main cusps at the OES, while five cuspules along the distal marginal ridge are traceable at the EDJ level on Tighenif 2's LP4 (Fig. 3). As observed on the LP3s, both Tighenif 1's LP4 roots display three fused branches with similar pulp morphology (contra Arambourg and Hoffstetter, 1963, who identified only two fused branches and pulp canals). On the other hand, the LP4 of Tighenif 2 shows four fused branches separated at the apex, with a deeply invaginated developmental groove (stage 4 following Turner II et al., 1991). This condition more closely approximates the mesial and distal 2R Tomes' root morphotype described by Wood et al. (1988), with a sub-rhomboidal mid-root cross-section and four distinct pulp canals.

Among the three isolated upper molars, only the pulp chamber occlusal morphology of the URM1/2 preserves indirect evidence of the cusp pattern (Fig. 1), while the preserved portion of the incomplete but unworn URM evidences the absence of accessory cusp or wrinkling (Fig. 3).

As pointed out in previous descriptions of this fossil sample (Arambourg and Hoffstetter, 1963), the crown of the lower molars is low, bearing five main cusps at the OES. At the EDJ, while the molars in Tighenif 1 do not

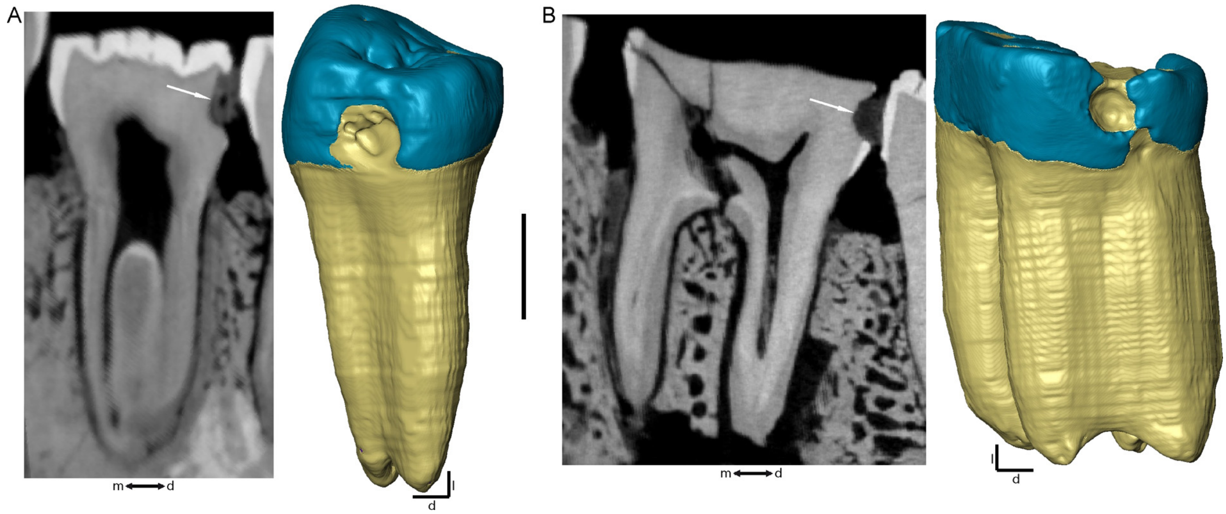

Fig. 2. Virtual mesiodistal cross-section through the central axis (left) and 3D rendering (right) of the LLP4 of Tighenif 2 (A) and of the LRM1 of Tighenif 1 (B) whose distal aspects exhibit the previously unreported evidence of a local decalcification involving both enamel and dentine (arrows), but not reaching the pulp cavity. These cavities represent in both cases an interproximal carious lesion. d: distal; l: lingual; m: mesial. Scale: 5 mm. Colour available online.
Fig. 2. Section mésio-distale virtuelle passant par l'axe central (gauche) et reconstruction 3D (droite) de la LLP4 de Tighenif 2 (A) et de la LRM1 de Tighenif 1 (B), dont les faces distales montrent des décalcifications locales encore non signalées précédemment affectant l'émail et la dentine (flèches), mais n'atteignant pas la cavité pulpaire. Ces cavités représentent dans les deux cas des lésions carieuses interproximales. d : distal ; l : lingual ; m : mésial. Échelle : 5 mm. Couleur disponible en ligne.

express any *tuberculum sextum* (C6) or *tuberculum intermedium* (C7), both the LM2 and LM3 of Tighenif 2 bear a hypoconulid-type C6, and all three molars also possess a C7 (of metaconulid-type in LM1 and of interconulid-type in LM2 and LM3). The mid-trigonid crest is expressed in both mandibles, even if it progressively weakens distally. More specifically, while this feature is not traceable in Tighenif 1 LM1s because of occlusal wear, it is detectable on the LM2s (stage 2, middle-middle type) and on both the LM1 (stage 2, middle-middle type) and the LM2 (stage 1, middle-middle type) of Tighenif 2. In Tighenif 1, the LM3s display a metameric variation in the expression of this feature. In this case, an interrupted ridge and a small crest running from the mesial marginal ridge towards the centre of the anterior fovea are present on the right side (stage 1, mesial marginal ridge-middle type), while a quite low but complete expression (stage 2, mesial-middle type) is found on the left side. Finally, the mid-trigonid crest is interrupted in the last molar of Tighenif 2 (stage 1, middle-middle type). A variable number of one to three wrinkles running distally from the protoconid towards the centre of the occlusal basin are present in all lower molars considered in this study, but only in the LM3 of Tighenif 2 a complete distal trigonid crest is fully expressed.

All lower molars possess two roots, the mesial one being constituted by two fused mesiobuccal and mesiolingual branches with a free apex, and the distal root showing either two branches (a distobuccal and a distolingual one with a free or fused apex) in the LM1s and LM2s, or a single one in the LM3s. In all cases, the pulp canals are always well distinct in each branch (Fig. 1).

As already noticed in the radiographic study realized by Arambourg and Hoffstetter (1963), in this fossil assemblage the molar pulp chamber volume proportionally increases distally. In this respect, while Tighenif 1 does not differ from the morphodimensional condition found in recent human populations (Kupczik and Hublin, 2010), Tighenif 2's LM2 and LM3 exhibit a rather expanded pulp cavity (see infra for tissue proportions).

3.2. Occlusal enamel thickness distribution

Site-specific enamel thickness variation has been comparatively rendered through a 3D topographic mapping of the crown in occlusal projection using a chromatic scale where thickness increases from dark-blue to red. Unfortunately, the degree of wear affecting most crowns strongly weakens the value of this analytical approach on the Tighenif's fossil assemblage. However, here this visualisation technique has been tentatively applied to the isolated fragmentary URM and to the relatively moderately worn LP3-M3 crowns of Tighenif 2 (Fig. S1 in Supplementary data).

While the occlusal surface of the LP3 shows two large patches of emerging dentine, both premolars apparently share a similar distribution pattern, the thicker enamel being found along the buccal side, as more distinctly detectable on the LP4. Similarly, as variably found in other fossil and recent humans (Kono and Suwa, 2008; Macchiarelli et al., 2013), the thickest enamel is set towards the distolingual and the distobuccal cusps, respectively on the upper and the lower molars.

3.3. Tooth tissue proportions: description and comparisons

Tooth tissue proportions of two isolated (LRI1 and LRI2) and eight in situ specimens (3 lower premolars and 8 molars) displaying only a slight to moderate degree of wear (from stage 2 to 4) are detailed in Table 1. However, despite

Table 1
Surface and volumetric estimates and dental tissue proportions of ten permanent teeth from Tighenif.
Tableau 1
Paramètres surfaciques et volumétriques et proportions des tissus chez dix dents permanentes de Tighenif.

	Position	Wear	V_e (mm^3)	V_d (mm^3)	V_p (mm^3)	V_t (mm^3)	V_p/V_t (mm^3)	V_{cd} (mm^3)	V_{cp} (mm^3)	V_{cdp} (mm^3)	V_c (mm^3)	SEDJ (mm^2)	V_{cdp}/V_c (%)	3D AET (mm)	3D RET
I1															
Isolated tooth	Lower right	3	40.84[a]	342.99[a]	15.80	399.63[a]	3.95[a]	86.42[a]	4.63	91.05[a]	131.89[a]	122.12[a]	69.03[a]	0.33[a]	7.43[a]
I2															
Isolated tooth	Lower right	3	45.20[a]	341.76[a]	27.45	414.41[a]	6.62[a]	86.14[a]	4.63	90.77[a]	135.97[a]	106.42[a]	66.76[a]	0.42[a]	9.45[a]
P3															
Tighenif 2	Lower left	3	101.96[a]	570.39[a]	53.77	726.12[a]	7.41[a]	191.21[a]	11.54	202.75[a]	304.71[a]	165.53[a]	66.54[a]	0.62[a]	10.49[a]
P4															
Tighenif 1	Lower left	4	88.58[a]	782.52[a]	33.38	904.48[a]	3.69[a]	178.69[a]	2.52	181.21[a]	269.79[a]	159.83[a]			
Tighenif 2	Lower left	3	169.43[a]	752.96[a]	68.26	990.64[a]	6.89[a]	217.55[a]	6.94	224.49[a]	393.91[a]	190.88[a]	56.99[a]	0.89[a]	14.61[a]
M1															
Tighenif 2	Lower left	4	278.19[a]	1302.91[a]	117.49	1698.59[a]	6.92[a]	449.99[a]	19.33	469.33[a]	747.52[a]	298.16[a]			
M2															
Tighenif 2	Lower left	3	373.06	1362.08	191.64	1926.78	9.95	480.15	22.27	502.43	875.49	312.54	57.39	1.19	15.01
M3															
Tighenif 1	Lower left	4	188.79[a]	1271.76[a]	77.51	1538.06[a]	5.04[a]	341.81[a]	4.73	346.54[a]	535.33[a]	246.50[a]			
	Lower right	3	203.12[a]	1260.04[a]	79.26	1542.42[a]	5.14[a]	341.10[a]	4.12	345.22[a]	548.34[a]	242.77[a]	62.96[a]	0.84[a]	11.93[a]
Tighenif 2	Lower left	2	372.24	969.36	175.57	1517.17	11.57	362.35	9.18	371.53	743.78	255.48	49.95	1.46	20.27

[a] Affected by occlusal wear.

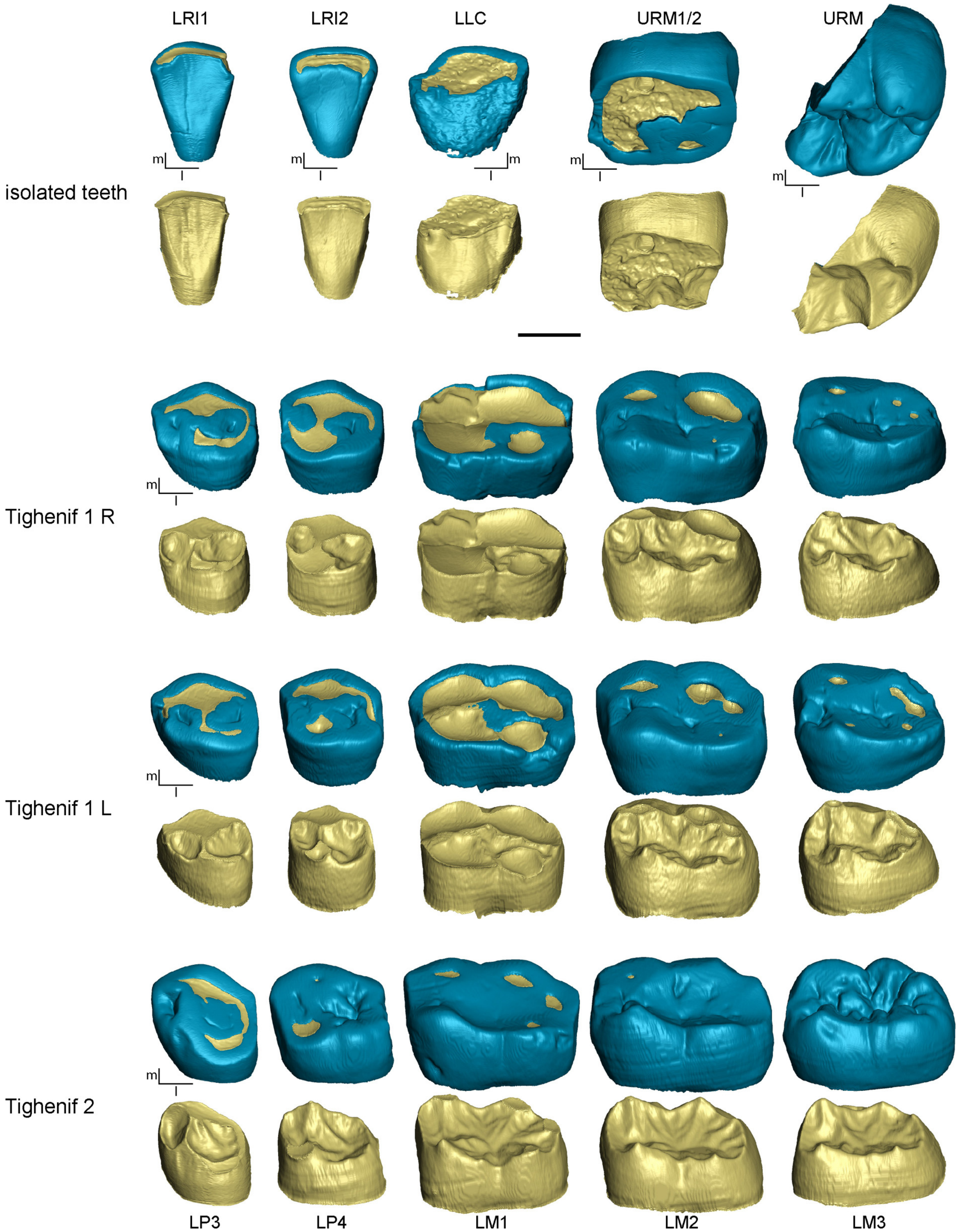
LRI1
LRI2
LLC
URM1/2
URM
isolated teeth
Tighenif 1 R
Tighenif 1 L
Tighenif 2
LP3
LP4
LM1
LM2
LM3

Table 2
Dental tissue proportions of the second and third lower molars comparatively assessed in Tighenif 2, Neanderthals (NEA), African fossil modern humans (AFMH) and extant humans (EH).

Tableau 2
Proportions des tissus dentaires des secondes et troisièmes molaires inférieures comparées chez Tighenif 2, les Néandertaliens (NEA), les humains modernes fossiles d'Afrique (AFMH) et les humains actuels (EH).

		V_p/V_t[a] (%)	V_{cdp}/V_c (%)	3D RET
LM2				
Tighenif 2		9.9	57.4	15.0
NEA (11)	Mean	7.6	57.1	15.4
	Range	5.7–9.2	51.0–64.2	11.9–20.9
AFMH (3)	Mean	11.3	53.4	17.6
	Range	9.1–12.6	50.4–56.6	14.7–19.9
EH (26)	Mean	4.7	51.0	20.2
	Range	3.1–8.1	42.7–57.3	12.6–40.7
LM3				
Tighenif 2		11.6	50.0	20.3
NEA (13)	Mean	7.1	58.1	16.2
	Range	5.5–9.6	47.2–68.6	12.7–21.8
AFMH (2)	Mean	13.6	51.0	19.1
	Range	11.7–15.5	49.3–52.7	16.9–21.3
EH (14)	Mean	4.5	49.4	21.6
	Range	2.4–6.7	44.7–55.4	17.8–27.8

AFMH: African fossil modern humans (Kupczik and Hublin, 2010); EH: extant humans (Olejniczak et al., 2008b; and original data); NEA: Neanderthals (Kupczik and Hublin, 2010; Macchiarelli et al., 2013; NESPOS Database, 2013; Olejniczak et al., 2008a).

[a] A sub-sample of specimens was used to calculate the ratio V_p/V_t (Table S1).

the exclusion of over 50% of the teeth detailed by μCT from this analysis, in most cases the values have yet to be considered as minimum estimates only, while of course the opposite is true for the percent ratio V_{cdp}/V_c, i.e, the percent of coronal volume that is dentine and pulp. While the pulp volume estimates (V_p and V_{cp}) are reliable in all investigated cases, uniquely the results pertaining to the LLM2 and LLM3 of Tighenif 2 have been used in the comparative analyses with other fossil and extant samples (Table 2).

The two isolated mandibular incisors, affected by a comparable degree of wear, show differences lower than 5% for most volumetric estimators, except for V_e, V_p and V_p/V_t, which are ca. 10%, 73% and 67.6% higher in the lateral incisor, respectively, while the EDJ area (SEDJ) is ca. 15% larger in the central one.

For all parameters, except V_p/V_t and V_{cp}, Tighenif 2's LP3 systematically shows lower values than its adjacent premolar. Mostly due to its lower amount of removed occlusal enamel, Tighenif 2's LP4 estimates tend to exceed those from its counterpart on Tighenif 1. However, as illustrated by the ratio V_p/V_t, the marked difference between the two teeth for the total volume of the pulp (V_p) should more likely reflect individual structural variation, given also their similarity for the variable V_d.

As noted above, most values pertaining to the Tighenif 2's LM1 should be considered as indicative only, even if its V_d and SEDJ estimates fit those provided by the less worn adjacent LM2. Overall, Tighenif 2's LM1 and LM2 estimates tend to exceed those of both Tighenif 1 and 2 third molars (Table 1). It is interesting to note that, despite a higher degree of wear found on the left side, both last molars of Tighenif 1 display comparable tissue proportions, except for the total volume of the enamel cap, which is of course, higher on the RM3. However, except for V_d and V_t, both series of data are systematically lower compared to the results from the slightly worn LLM3 of Tighenif 2.

As shown by the ratio V_p/V_t, Tighenif 2 exhibits a distal trend in the volumetric expansion of the molar pulp cavity, nearly double from the LM1 to the LM3, while Tighenif 1's LM3s have a much smaller pulp volume compared to their counterparts in Tighenif 2. Limitedly to the crown, Tighenif 2's LM3 displays a lower V_{cdp}/V_c ratio and higher 3D AET and 3D RET indices compared to its LM2 and to Tighenif 1's LM3s.

Comparative tissue proportions for the second and third lower molars of Tighenif 2, Neanderthals (NEA), European Upper Paleolithic humans (EUPH), African fossil modern humans (AFMH) and extant humans (EH) are shown in Table 2. In both Tighenif's molars, the V_p/V_t ratio exceeds both the Neanderthal and the extant human values, but approximates the African fossil modern human estimates (Fig. S2A in Supplementary data). For the V_{cdp}/V_c ratio, while the LM2 of the Algerian specimen falls within the Neanderthal range, it slightly exceeds the figures of the fossil modern and extant human samples (Fig. S2B in Supplementary data). Conversely, in the present comparative context, the same ratio is poorly discriminant with regards to Tighenif 2's LM3 (Fig. S2B in Supplementary data), an evidence which also concerns the 3D RET estimates of Tighenif 2's LM2 and LM3 (Fig. S2C in Supplementary data).

Finally, the results of the adjusted Z-score analysis performed for the three indices V_p/V_t, V_{cdp}/V_c, and 3D RET are illustrated in Fig. 4. Except for V_p/V_t in the extant human sample, both Tighenif 2's molars approximate the conditions expressed by Neanderthals and African fossil humans, showing the closest affinities with the latter group (notably for the LM3).

3.4. *Comparative shape analysis of the enamel-dentine junction (EDJ)*

Based on the Procrustes shape coordinates obtained by the geometric morphometric analysis of the EDJ, the results of the between-group principal component analysis of the LM2s and LM3s (cf. Section 2. Materials and methods of analysis) are shown in Fig. 5. In this case, the three selected molars representing Tighenif have been compared to the

Fig. 3. 3D virtual reconstruction of the outer crown surface (top row) and of the related enamel-dentine junction (bottom row) of five isolated teeth from Tighenif and of 15 crowns virtually extracted from the mandibles Tighenif 1 and 2, in occlusal-lingual view. To make the comparison easier, the right LP3-LM3 of Tighenif 1 (Tighenif 1 R) have been mirrored. l: lingual; m: mesial. Scale: 5 mm. Colour available online.

Fig. 3. Reconstructions virtuelles 3D de la surface externe de l'émail (rangée supérieure) et de la jonction émail-dentine (rangée inférieure) de cinq dents isolées de Tighenif et de 15 couronnes virtuellement extraites des mandibules Tighenif 1 et 2, en vue occluso-linguale. Pour faciliter la comparaison, les LP3-LM3 droites de Tighenif 1 (Tighenif 1 R) ont été inversées. l : lingual ; m : mésial. Échelle : 5 mm. Couleur disponible en ligne.

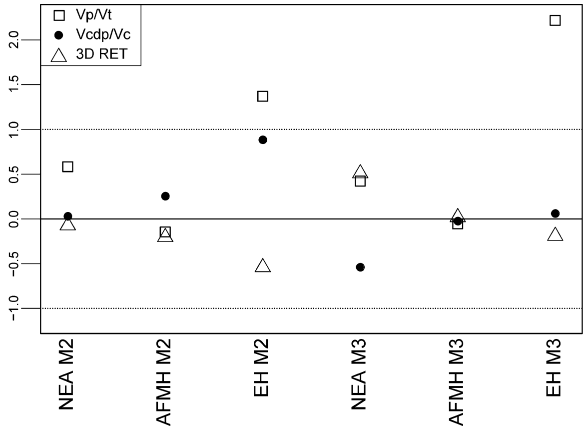

Fig. 4. Adjusted Z-score analysis of three indices describing tissue proportions assessed in the second and third lower molars of Tighenif 2 and compared to the variation expressed by Neanderthals (NEA), African fossil modern humans (AFMH), and extant humans (EH). The central and dotted lines correspond to the mean and to the 95% limit of variation of the comparative samples, respectively, while the symbols represent the position of Tighenif 2.

Fig. 4. Analyse des écarts réduits ajustés de trois indices décrivant les proportions des tissus, estimés pour la seconde et la troisième molaires inférieures de Tighenif 2, comparés à la variation exprimée par les Néandertaliens (NEA), les humains modernes fossiles d'Afrique (AFMH) et les humains actuels (EH). La ligne centrale et les lignes en pointillés correspondent respectivement à la moyenne et aux limites de variation à 95 % des trois échantillons comparatifs fossiles et actuels, tandis que les symboles représentent la position de Tighenif 2.

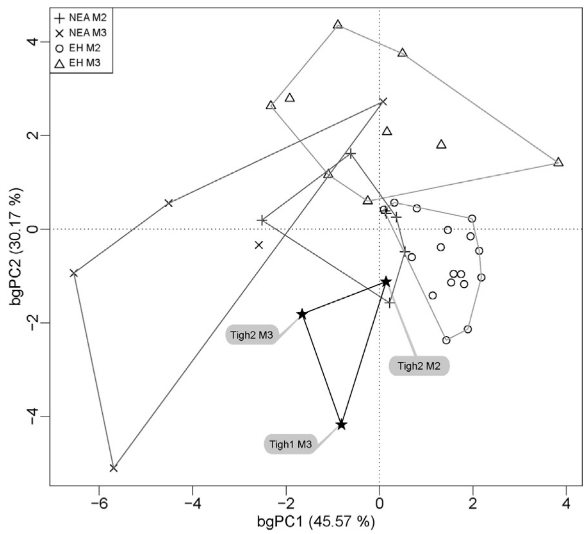

Fig. 5. Between-group PCA (bgPCA) of the Procrustes shape coordinates representing the global enamel-dentine junction conformation of the second and third lower molars of Tighenif 1 (LRM3) and Tighenif 2 (LLM2 and LLM3), Neanderthals (NEA) and extant humans (EH).

Fig. 5. Analyse en composantes principales intergroupe, réalisée à partir des coordonnées Procrustes représentant la conformation globale de la jonction émail-dentine des secondes et troisièmes molaires inférieures de Tighenif 1 (LRM3) et Tighenif 2 (LLM2 et LLM3), Néandertaliens (NEA) et humains actuels (EH).

Table 3
P-values of pairwise group differences based on 10,000 permutations.
Tableau 3
Probabilités des différences entre groupes par comparaisons appariées basées sur 10 000 permutations.

	NEA M2	NEA M3	EH M2	EH M3
NEA M3	0.071			
EH M2	0.090	0.001**		
EH M3	0.144	0.001**	0.004*	
Tighenif	0.057	0.043*	0.030*	0.005**

The symbols * and ** indicate the differences which are significant for $P \leq 0.05$ and ≤ 0.01, respectively.

similar variation expressed by 12 Neanderthals (NEA) and 26 extant humans (EH).

As a whole, the Tighenif's LM3s fall apart from both comparative samples, but closer to the Neanderthal figures, while the LM2 from Tighenif 2 more closely nears the Neanderthal conformation pattern. Indeed, similarly to Neanderthals and distinctly from the extant human condition, Tighenif lower molars present a buccolingually straighter talonid and a more mesiodistally elongated crown bearing a higher metaconid dentine horn. Accordingly, the results of the permutation tests indicate that these endostructural shape differences are all statistically significant, except between Tighenif and Neanderthals for the LM2 (Table 3).

4. Discussion

A previous analysis of three upper deciduous molars from the Tighenif fossil assemblage (two Um1s and one Um2, likely from the same individual) has comparatively assessed their crown tissue proportions and enamel thickness topography. The results from the 2-3D measurements indicate that their structural signature better approximates the modern human figures rather than the typical Neanderthal condition (Zanolli et al., 2010). However, a preliminary investigation of the degree of parallelism between deciduous and permanent crown signatures in tracking the taxon-related structural changes in tissue proportions throughout the last million years has revealed a more complex pattern (Macchiarelli et al., 2013). In this latter study, the isolated Um2 and the virtually unworn LM3 of Tighenif 2 were compared for their structural organization to similar evidence from Javanese *H. erectus*, Middle Pleistocene *H. heidelbergensis* from Tautavel (France), Neanderthals, and extant humans. Interestingly, in terms of crown tissue proportions, the pattern displayed by the North African and European *H. heidelbergensis* specimens represented in the study did not fully overlap, the tooth pair from Tighenif expressing a deciduous *vs.* permanent molar structural condition closer to the Neanderthal pattern (Macchiarelli et al., 2013).

By investigating 22 permanent elements from the Tighenif's dental assemblage, the present high-resolution study has significantly enlarged the amount of information currently available on *H. heidelbergensis* tooth structural organization, revealing a previously unreported mosaic of primitive and derived features and a certain degree of variation characterizing this North African fossil sample.

Virtually along the entire root, the pulp cavity of both isolated mandibular incisors from Tighenif displays an ovoid cross-sectional contour. This pattern differs from the condition recently reported for the Early Pleistocene LI2 from Atapuerca Sima del Elefante, Spain (Prado-Simón et al., 2012a) and also found in the lower incisors of the Neanderthal partial skeleton from Regourdou, France (Macchiarelli et al., 2013), both rather characterized by a mesiodistally flattened radicular canal. However, given the variability expressed by this feature in our microtomographic-based reference database of extant human permanent lower incisors and the small amount of available comparative information (Le Cabec et al., 2012; Prado-Simón et al., 2012a), its potential informative value for taxonomic and phylogenetic assessment still requires additional research.

The EDJ of Tighenif 2's LLP4 exhibits a mesiodistally extended talonid with five cuspules lying along the distal marginal ridge, a morphology reminiscent of the ancestral molar-like configuration observed in early hominins (Braga et al., 2010). Moreover, all the premolars exhibit complex 2R Tomes' root morphologies interpreted as a rather primitive condition (Prado-Simón et al., 2012a, 2012b; Wood et al., 1988). In fact, this pattern is found in *H. ergaster* (e.g., KNM-ER 730; Wood et al., 1988), early *Homo* from Atapuerca Sima del Elefante (ATE9-1; Prado-Simón et al., 2012a, 2012b), *H. erectus* from Zhoukoudian (e.g., GI-60; Weidenreich, 1937) and Sangiran (e.g., Sb 8103; Kaifu et al., 2005). Conversely, European *H. heidelbergensis*, Neanderthals and modern humans more commonly show a single root morphology (Prado-Simón et al., 2012b; Wood et al., 1988).

Compared to the inner signature characterizing the premolars, the EDJ of the lower molars displays a set of nonmetric traits more frequently found in recent humans than in Neanderthals. In particular, Tighenif 2's LM2 and LM3 exhibit a hypoconulid-type *tuberculum sextum*, a feature never observed in Lower Pleistocene hominins or in Neanderthals, where the fovea-type is predominant (Skinner et al., 2008). Conversely, whenever a *tuberculum intermedium* is expressed, the interconulid- and metaconulid-type seen in the Tighenif's molars seem to be quite common in the human lineage (Skinner et al., 2008).

At the EDJ, the Tighenif's molars show a comparable number of cases scored as 1 (3/7 cases) and 2 (4/7) for the degree of expression of the mid-trigonid (metaconid) crest, while the first condition is extremely rare in Neanderthals (1: 1.4%; 2: 39.7%) and also less frequent than the second one in modern humans (11.8% vs. 35.3%) (Bailey et al., 2011; Macchiarelli et al., 2006). The exclusively middle-middle type origin of this feature recorded on Tighenif also more closely approximates the modern human frequencies (Bailey et al., 2011). In this respect, it is noteworthy that the endostructural exploration of the *H. heidelbergensis* mandible from Mauer, Germany, revealed no expression of the mid-trigonid crest (Bailey et al., 2011), a condition also shown by the LM1 of the North African late Middle Pleistocene specimen Irhoud 3 and, more generally, by recent humans (Bailey et al., 2011).

Similarly to the condition reported for African fossil modern humans (Hublin et al., 2012; Kupczik and Hublin, 2010), the lower molars from Tighenif display relatively large pulp cavities, but with a rather high root bifurcation and well-separated pulp canals. This pattern contrasts with the typical (and exclusive) Neanderthal single, pyramidal roots, where the commonly taurodontic pulp cavity extends into the apex before branching out into short root canals (Kupczik and Hublin, 2010; Macchiarelli et al., 2006, 2008, 2013).

Also for tooth crown tissue proportions, the lower permanent molars of Tighenif (Tighenif 2's LM2 and LM3) exhibit a blend of Neanderthal- and modern-like features. More precisely, the LM2 fits the average Neanderthal condition represented by a high crown dentine percent value and an intermediate to relatively thick enamel (Kupczik and Hublin, 2010; Macchiarelli et al., 2013; Olejniczak et al., 2008a). Conversely, because of its moderately developed crown dentine core and relatively thick enamel, the Algerian LM3 more closely approximates the fossil and recent modern human condition (Kupczik and Hublin, 2010; Olejniczak et al., 2008a). However, the morphometric assessment of the EDJ molar conformation performed on the Tighenif 1's RM3 and Tighenif 2's LM2 and LM3 highlighted their relatively distinct 3D pattern with respect to the variation expressed by the Neanderthal and extant human comparative samples used in this study, even if the Algerian specimens reveal a closer affinity with the Neanderthal figures. Nonetheless, whenever both the pulp chamber conformation and its relative position with respect to the EDJ are examined, the molars from Tighenif better approximate the modern human condition (Zanolli, 2012).

Finally, as hypothesized on the basis of the morphodimensional similarities recorded among some Middle Pleistocene North African dentognathic series (Bräuer, 2012), the fact that the Tighenif molars bear a resemblance in dental structural organization to the Upper Pleistocene Aterian assemblage (Hublin et al., 2012; Kupczik and Hublin, 2010) points to a certain degree of evolutionary continuity at macro-regional scale and/or to a long-standing contribution of the area to the establishment of the modern-like tooth morphology.

5. Conclusive remarks

The combination of inner morphostructural characters found in the permanent tooth elements of the Tighenif fossil assemblage supports the suggestion that this Middle Pleistocene North African deme is probably part of the stem group leading to the Neanderthal, Denisovan and modern human allotaxa (Stringer, 2012). While the structural signature virtually extracted from the three deciduous molars represented in this sample more closely approximates the modern human condition rather than the Neanderthal figures (Zanolli et al., 2010), the present analysis of the permanent dentition highlights a more complex pattern, combining unique, primitive, Neanderthal-like and modern human-like features, notably at the EDJ and pulp levels. In this regard, the structural affinity noted with the figures reported for some Aterian samples (Hublin et al., 2012;

Kupczik and Hublin, 2010) deserves more specific research aimed to precise the nature, extent and meaning of such similarities.

Besides some severe dental wear- or traumatic-related inflammatory bony reactions, dentognathic pathologies are relatively rare in the human fossil record (Gracia-Téllez et al., 2013; Martinón-Torres et al., 2011). Tooth decays have mostly been detected in Neanderthals and fossil modern humans (Lalueza et al., 1993; Lebel and Trinkaus, 2001, 2002; Tillier et al., 1995; Trinkaus et al., 2000; rev. in Walker et al., 2011), even if one of the most remarkable cases is represented by the Middle Pleistocene *H. heidelbergensis* specimen Kabwe 1, Zambia, exhibiting rampant dental caries with 10 of 16 maxillary teeth affected (Lukacs, 2012). Thanks to the use of high-resolution virtual imaging techniques, the present finding of two previously unreported interproximal carious lesions in the postcanine tooth rows of Tighenif 1 and 2 thus adds new evidence to the rather scanty Middle Pleistocene record available so far, and also supports the call of Walker et al. (2011) that the extension of similar research to the human fossil record should very likely expose more undetected dental pathologies, notably in association with extensive occlusal wear (Hillson, 2008).

Acknowledgements

The authors sincerely thanks C. Argot and H. Lelièvre for having granted access to the fossil specimens of Tighenif discussed in this paper, as well as for their support during all phases of our study. The microtomographic record has been realized at the Centre de Microtomographie (CdM) of the Univ. of Poitiers thanks to the support of R. Macchiarelli. For scientific collaboration, we sincerely acknowledge P. Bayle, L. Bondioli, J. Braga, A. Coppa, M.C. Dean, F.E. Grine, R. Macchiarelli, L. Mancini, B. Maureille, C. Tuniz. Research supported by the MNHN, the Société des Amis du Musée de l'Homme, the DAAD, the CNRS, the Univ. of Poitiers, the Neanderthal Studies Professional Online Service (NESPOS) Society. We note that the present version greatly benefited from the comments provided by two anonymous reviewers.

Appendix A. Supplementary data

Supplementary data associated with this article can be found, in the online version, at http://dx.doi.org/10.1016/j.crpv.2013.06.004.

References

Antón, S.C., 2003. Natural history of *Homo erectus*. Yearb. Phys. Anthropol. 46, 126–170.
Antón, S.C., Spoor, F., Fellmann, C.D., Swisher III, C.C., 2007. Defining *Homo erectus*: size considered. In: Henke, W., Tattersall, I. (Eds.), Handbook of Paleoanthropology. Springer, New York, pp. 1655–1695.
Arambourg, C., 1954. L'hominien fossile de Ternifine (Algérie). C. R. Acad. Sci. Paris 239, 893–895.
Arambourg, C., 1955. A recent discovery in human paleontology: *Atlanthropus* of Ternifine (Algeria). Am. J. Phys. Anthropol. 13, 191–201.
Arambourg, C., 1957. Récentes découvertes de paléontologie humaine réalisées en Afrique du Nord française (L'*Atlanthropus* de Ternifine – L'Hominien de Casablanca). In: Clark, J.D., Cole, S. (Eds.), Proceedings of the Third Panafrican Congress on Prehistory. Chatto and Windus, London, pp. 186–194.
Arambourg, C., Hoffstetter, R., 1954. Découverte en Afrique du Nord de restes humains du Paléolithique inférieur. C. R. Acad. Sci. Paris 239, 72–74.
Arambourg, C., Hoffstetter, R., 1963. Le gisement de Ternifine. Arch. Inst. Paleontol. Hum. 32, 1–190.
Bailey, S.E., Skinner, M.M., Hublin, J.J., 2011. What lies beneath? An evaluation of lower molar trigonid crest patterns based on both dentine and enamel expression. Am. J. Phys. Anthropol. 145, 505–518.
Bayle, P., Macchiarelli, R., Trinkaus, E., Duarte, C., Mazurier, A., Zilhão, J., 2010. Dental maturational pattern and dental tissue proportions in the early Upper Paleolithic child from Abrigo do Lagar Velho, Portugal. Proc. Natl. Acad. Sci. U S A 107, 1338–1342.
Bermúdez de Castro, J.M., Martinón-Torres, M., Gómez-Robles, A., Prado-Simón, L., Martin-Francés, L., Lapresa, M., Olejniczak, A.J., Carbonell, E., 2011. Early Pleistocene human mandible from Sima del Elefante (TE) cave site in Sierra de Atapuerca (Spain): a comparative morphological study. J. Hum. Evol. 61, 12–25.
Bondioli, L., Bayle, P., Dean, C., Mazurier, A., Puymerail, L., Ruff, C., Stock, J.T., Volpato, V., Zanolli, C., Macchiarelli, R., 2010. Morphometric maps of long bone shafts and dental roots for imaging topographic thickness variation. Am. J. Phys. Anthropol. 142, 328–334.
Braga, J., Thackeray, J.F., Subsol, G., Kahn, J.L., Maret, D., Treil, J., Beck, A., 2010. The enamel-dentine junction in the postcanine dentition of *Australopithecus africanus*: Intra-individual metameric and antimeric variation. J. Anat. 216, 62–79.
Bräuer, G., 2012. Middle Pleistocene diversity in Africa and the origin of modern humans. In: Hublin, J.J., McPherron, S.P. (Eds.), Modern Origins: A North African Perspective. Springer, Dordrecht, pp. 221–240.
Coleman, M.N., Colbert, M.W., 2007. Technical note: CT thresholding protocols for taking measurements on three-dimensional models. Am. J. Phys. Anthropol. 133, 723–725.
Fajardo, R.J., Ryan, T.M., Kappelman, J., 2002. Assessing the accuracy of high resolution X-ray computed tomography of primate trabecular bone by comparisons with histological sections. Am. J. Phys. Anthropol. 118, 1–10.
Geraads, D., Hublin, J.J., Jaeger, J.J., 1986. The Pleistocene hominid site of Ternifine Algeria: new results on the environment, age, and human industries. Quat. Res. 25, 380–386.
Gracia-Téllez, A., Arsuaga, J.L., Martínez, I., Martín-Francés, L., Martinón-Torres, M., Bermúdez de Castro, J.M., Bonmatí, A., Lira, J., 2013. Orofacial pathology in *Homo heidelbergensis*: the case of Skull 5 from the Sima de los Huesos site (Atapuerca, Spain). Quat. Int. 295, 83–93.
Hillson, S.W., 2001. Recording dental caries in archaeological human remains. Int. J. Osteoarchaeol. 11, 249–289.
Hillson, S.W., 2008. The current state of dental decay. In: Irish, J.D., Nelson, G. (Eds.), Technique and Application in Dental Anthropology. Cambridge University Press, Cambridge, pp. 111–135.
Howell, F.C., 1960. European and Northwest African Middle Pleistocene hominids. Curr. Anthropol. 1, 195–232.
Hublin, J.J., Verna, C., Bailey, S., Smith, T.M., Olejniczak, A.J., Sbihi-Alaoui, F.Z., Zouak, M., 2012. Dental evidence from the Aterian human populations of Morocco. In: Hublin, J.J., McPherron, S.P. (Eds.), Modern Origins: A North African Perspective. Springer, Dordrecht, pp. 189–204.
Kaifu, Y., Baba, H., Aziz, F., Indriati, E., Schrenk, F., Jacob, T., 2005. Taxonomic affinities and evolutionary history of the Early Pleistocene hominins of Java: dentognathic evidence. Am. J. Phys. Anthropol. 128, 709–726.
Kono, R., 2004. Molar enamel thickness and distribution patterns in extant great apes and humans: new insights based on a 3-dimensional whole crown perspective. Anthropol. Sci. 112, 121–146.
Kono, R., Suwa, G., 2008. Enamel distribution patterns of extant human and hominoid molars: occlusal versus lateral enamel thickness. Bull. Natl. Mus. Nat. Sci. Ser. D 34, 1–9.
Kupczik, K., Hublin, J.J., 2010. Mandibular molar root morphology in Neanderthals and Late Pleistocene and recent *Homo sapiens*. J. Hum. Evol. 59, 525–541.
Lalueza, C., Pérez-Pérez, A., Chimenos, E., Maroto, J., Turbón, D., 1993. Estudi radiogràfic i microscòpic de la mandíbula de Banyoles: patologies i estat de conservació. In: Maroto, J. (Ed.), La mandíbula de Banyoles en el context dels fossils humans del Pleistocè. Sèrie Monogràfica 13. Centre d'Investigacions Arqueològiques de Girona, Girona, pp. 135–144.
Lebel, S., Trinkaus, E., 2001. New discoveries of Middle Paleolithic human remains from the "Bau de l'Aubésier (Vaucluse, France)". Bull. Mem. Soc. Anthropol. Paris 13, 15–21.

Lebel, S., Trinkaus, E., 2002. Short Note. A carious Neandertal molar from the Bau de l'Aubesier, Vaucluse, France. J. Archaeol. Sci. 29, 555–557.

Le Cabec, A., Kupczik, K., Gunz, P., Braga, J., Hublin, J.-J., 2012. Long anterior mandibular tooth roots in Neanderthals are not the result of their large jaws. J. Hum. Evol. 63, 667–681.

Le Gros Clark, W.E., 1964. The fossil evidence for human evolution: an introduction to the study of palaeoanthropology, second ed. University of Chicago Press, Chicago.

Lukacs, J.R., 2012. Oral health in past populations: Context, concepts and controversies in the study of dental disease. In: Grauer, A.L. (Ed.), A Companion to Paleopathology. Blackwell, Chichester, pp. 553–582.

Macchiarelli, R., Bayle, P., Bondioli, L., Mazurier, A., Zanolli, C., 2013. From outer to inner structural morphology in dental anthropology. The integration of the third dimension in the visualization and quantitative analysis of fossil remains. In: Scott, G.R., Irish, J.D. (Eds.), Anthropological Perspectives on Tooth Morphology. Genetics, Evolution, Variation. Cambridge University Press, Cambridge, pp. 250–277.

Macchiarelli, R., Bondioli, L., Debénath, A., Mazurier, A., Tournepiche, J.F., Birch, W., Dean, M.C., 2006. How Neanderthal molar teeth grew. Nature 444, 748–751.

Macchiarelli, R., Bondioli, L., Mazurier, A., 2008. Virtual dentitions: touching the hidden evidence. In: Irish, J.D., Nelson, G.C. (Eds.), Technique and Application in Dental Anthropology. Cambridge University Press, Cambridge, pp. 426–448.

Macchiarelli, R., Mazurier, M., Illerhaus, B., Zanolli, C., 2009. *Ouranopithecus macedoniensis*: virtual reconstruction and 3D analysis of a juvenile mandibular dentition (RPl-82 and RPl-83). Geodiversitas 31, 851–863.

Martinón-Torres, M., Martín-Francés, L., Gracia, A., Olejniczak, A.J., Prado-Simón, L., Gómez-Robles, A., Lapresa, M., Carbonell, E., Arsuaga, J.L., Bermúdez de Castro, J.M., 2011. Early Pleistocene human mandible from Sima del Elefante (TE) cave site in Sierra de Atapuerca (Spain): a palaeopathological study. J. Hum. Evol. 61, 1–11.

Maureille, B., Rougier, H., Houët, F., Vandermeersch, B., 2001. Les dents inférieures du néandertalien Regourdou 1 (site de Regourdou, commune de Montignac, Dordogne) : analyses métriques et comparatives. Paleo 13, 183–200.

Mitteroecker, P., Bookstein, F.L., 2011. Linear discrimination, ordination, and the visualization of selection gradients in modern morphometrics. Evol. Biol. 38, 100–114.

Mounier, A., Marchal, F., Condemi, S., 2009. Is *Homo heidelbergensis* a distinct species? New insight on the Mauer mandible. J. Hum. Evol. 56, 219–246.

NESPOS Database, 2013. Neanderthal studies professional online service. http://www.nespos.org

Olejniczak, A.J., Smith, T.M., Feeney, R.N.M., Macchiarelli, R., Mazurier, A., Bondioli, L., Rosas, A., Fortea, J., de la Rasilla, M., Garcia-Tabernero, A., Radovčić, J., Skinner, M.M., Toussaint, M., Hublin, J.-J., 2008a. Dental tissue proportions and enamel thickness in Neandertal and modern human molars. J. Hum. Evol. 55, 12–23.

Olejniczak, A.J., Tafforeau, P., Feeney, R.N.M., Martin, L.B., 2008b. Three-dimensional primate molar enamel thickness. J. Hum. Evol. 54, 187–195.

Prado-Simón, L., Martinón-Torres, M., Baca, P., Gómez-Roblez, A., Lapresa, M., Carbonell, E., Bermúdez de Castro, J.M., 2012a. A morphological study of the tooth roots of the Sima del Elefante mandible (Atapuerca, Spain): a new classification of the teeth – biological and methodological considerations. Anthropol. Sci. 120, 61–72.

Prado-Simón, L., Martinón-Torres, M., Baca, P., Olejniczak, A.J., Gómez-Robles, A., Lapresa, M., Arsuaga, J.L., Bermúdez de Castro, J.M., 2012b. Three-dimensional evaluation of root canal morphology in lower second premolars of Early and Middle Pleistocene human populations from Atapuerca (Burgos, Spain). Am. J. Phys. Anthropol. 147, 452–461.

R Development Core Team, 2013. R: a language and environment for statistical computing. http://www.R-project.org

Rightmire, G.P., 1990. The Evolution of *Homo erectus*. Cambridge University Press, New York.

Schlager, S., 2013. Morpho: calculations and visualizations related to geometric morphometrics. R package version 0.23.3 (http://sourceforge.net/projects/morpho-rpackage/?source=directory).

Schneider, C.A., Rasband, W.S., Eliceiri, K.W., 2012. NIH Image to ImageJ: 25 years of image analysis. Nat. Meth. 9, 671–675.

Schwartz, J.H., Tattersall, I., 2000. The human chin revisited: what is it and who has it? J. Hum. Evol. 38, 367–409.

Schwartz, J.H., Tattersall, I., 2003. The human fossil record. Craniodental morphology of genus *Homo* (Africa and Asia), vol. 2. Wiley-Liss, Hoboken.

Schwartz, J.H., Tattersall, I., 2005. The human fossil record. Craniodental morphology of early hominids (genera *Australopithecus*, *Paranthropus*, *Orrorin*), and overview, vol. 4. Wiley-Liss, Hoboken.

Schwartz, J.H., Tattersall, I., 2010. Fossil evidence for the origin of *Homo sapiens*. Yearb. Phys. Anthropol. 53, 94–121.

Scolan, H., Santos, F., Tillier, A.M., Maureille, B., Quintard, A., 2011. Des nouveaux vestiges néanderthaliens à Las Pélénos (Monsempron-Libos, Lot-et-Garonne, France). Bull. Mem. Soc. Anthropol. Paris 24, 69–95.

Skinner, M.M., Wood, B.A., Boesch, C., Olejniczak, A.J., Rosas, A., Smith, T.M., Hublin, J.J., 2008. Dental trait expression at the enamel-dentine junction of lower molars in extant and fossil hominoids. J. Hum. Evol. 54, 173–186.

Smith, H.B., 1984. Patterns of molar wear in hunter-gatherers and agriculturalists. Am. J. Phys. Anthropol. 63, 39–56.

Spoor, F., Zonneveld, F., Macho, G.A., 1993. Linear measurements of cortical bone and dental enamel by computed tomography: applications and problems. Am. J. Phys. Anthropol. 91, 469–484.

Stringer, C., 2012. The status of *Homo heidelbergensis* (Schoetensack 1908). Evol. Anthropol. 21, 101–107.

Tillier, A.M., 1980. Les dents d'enfant de Ternifine (Pléistocène moyen d'Algérie). L'Anthropologie 84, 413–421.

Tillier, A.M., Arensburg, B., Rak, Y., Vandermeersch, B., 1995. Middle Palaeolithic dental caries: new evidence from Kebara (Mount Carmel, Israel). J. Hum. Evol. 29, 189–192.

Trinkaus, E., Smith, R.J., Lebel, S., 2000. Dental caries in the Aubesier 5 Neandertal primary molar. J. Archaeol. Sci. 27, 1017–1021.

Turner II, C.G., Nichol, C.R., Scott, G.R., 1991. Scoring procedures for key morphological traits of the permanent dentition: the Arizona State University Dental Anthropology System. In: Kelley, M., Larsen, C. (Eds.), Advances in Dental Anthropology. Wiley-Liss, New York, pp. 13–31.

Walker, M.J., Zapata, J., Lombardi, A.V., Trinkaus, E., 2011. New evidence of dental pathology in 40,000-year-old Neandertals. J. Dent. Res. 90, 428–432.

Weidenreich, F., 1937. The dentition of *Sinanthropus pekinensis*: a comparative odontography of the hominids. Palaeontol. Sin. Ser. D 1, 1–180.

Wood, B.A., Abbot, S.A., Uytterschaut, H., 1988. Analysis of the dental morphology of Plio-Pleistocene hominids. IV. Mandibular postcanine root morphology. J. Anat. 156, 107–139.

Zanolli, C., 2012. Comparative tooth crown endostructural morphology in two penecontemporaneous samples of Indonesian *H. erectus* (Sangiran) and African *H. heidelbergensis* (Tighenif). Proc. Europ. Soc. Hum. Evol. 1, 196 (abstract).

Zanolli, C., Bayle, P., Macchiarelli, R., 2010. Tissue proportions and enamel thickness distribution in the early Middle Pleistocene human deciduous molars from Tighenif, Algeria. C. R. Palevol. 9, 341–348.

Zanolli, C., Bondioli, L., Mancini, L., Mazurier, A., Widianto, H., Macchiarelli, R., 2012. Two human fossil deciduous molars from the Sangiran Dome (Java, Indonesia): outer and inner morphology. Am. J. Phys. Anthropol. 147, 472–481.

Zanolli, C., Mazurier, A., Grimaud-Hervé, D., Macchiarelli, R., 2009. Les restes dentaires humains de la base du Pléistocène moyen de Tighennif, Algérie : révision d'étude par microtomographie à haute résolution. Bull. Mem. Soc. Anthropol. Paris 21, 204 (abstract).